

GM TUBE BETA-PARTICLE DETECTION EFFICIENCY CALCULATIONS

K. Vaziri

April 21, 1993

I. INTRODUCTION

The amount of released activated air from the target areas is monitored using a thin 1.75" diameter end-window GM tube installed inside a thick-walled lead canister¹ (see Figure 1). Several different isotopes were identified in the grab-sample taken from the APO stack. These isotopes emit different combinations of positrons, electrons and gamma-rays. To convert the count rate from a GM tube to activity (in Curies), the detection efficiency of the tube is required.

Detection efficiency of the GM tubes depends on the energy and type of incident radiation. Gas-filled detectors generally have reasonably good intrinsic efficiency ($\epsilon \approx 1$) for charged particles, but not for photons. The intrinsic efficiency of GM tubes to gamma rays is <0.01 and is a decreasing function of photon energy. In the following sections the calculation of the parameters used in determining the beta-particle detection efficiency of GM tubes (N1002/8767 "pancake" GM Tube²) used in our measurements are described.

II. CALCULATIONS

The GM tube's detection efficiency was calculated using

$$\epsilon_{GM} = f_{geom} \times f_{dt} \times f_{bksct} \times f_{\beta^+} \times f_{slf_abs} \times f_{trans} .$$

The terms in the above equation will be described in the following sub-sections and the method of calculation of each one will be presented.

Geometry factor f_{geom}

The geometry factor is defined as the fraction of the total solid angle subtended by a source to a detector aperture. The solid angle presented by an extended cylindrical source to a circular aperture detector was approximated by calculating the solid angle presented by a disk source and a circular aperture detector (see Figure 2)^{3,4} the same as the GM tube used in the study;

$$f_{geom} = G_p \left\{ 1 - \frac{3}{8} b^2 \left[\frac{H(H+D)}{D^4} \right] \right\},$$

where b is the radius of the source, H is the distance between the source and detector and D is given by

$$D = \sqrt{H^2 + a^2} ,$$

where a is the radius of the detector aperture. G_p is the fractional solid angle for a point source on the axis of a circular aperture detector given by

$$G_p = \frac{1}{2} \left[\frac{a^2}{D(D+H)} \right].$$

Dead time correction f_{dt}

The GM tube and its associated electronics have a characteristic pulse resolving time or dead time that is related to the time required to process individual detected events. This dead time causes loss of detected events, but it can be corrected for if the pulse width and the detected count rate are known, using

$$R_{true} = \frac{R_d}{1 - R_d \tau},$$

where R_{true} is the true count rate, R_d is the detected count rate and τ is the resolving time. The signal out of the GM tube and after processing had a maximum width of 70 μ -seconds. The ratio R_d / R_{true} was used as f_{dt} .

Backscattering f_{bkscf}

Large-angle deflection of beta-particles along their track is the phenomenon of back scattering. The amount of back scattering is dependent on the atomic number and thickness of the scatterer and the beta-particle energy⁵. Back scattering of beta-particles from the sample and its container increases the sample counting rate and can amount to 10-40 percent of the total counting rate. The back scattering fraction is calculated using

$$\eta = \frac{a_1}{1 + a_2 \tau^{a_3}},$$

where τ is the kinetic energy of the electron in units of electron rest mass (0.511 MeV) and a_i is target dependent and given by

$$\begin{aligned} a_1 &= b_1 \exp(-b_2 Z^{-b_3}), \\ a_2 &= b_4 + b_5 Z^{-b_6}, \\ a_3 &= b_7 - \frac{b_8}{Z}. \end{aligned}$$

The constants b_i were obtained from fitting to a large set of experimental data ranging from about 50 keV up to 22 MeV in energy and atomic number from 6 to 92:

$$\begin{aligned}
b_1 &= 1.15 \pm 0.06 & b_2 &= 8.35 \pm 0.25 \\
b_3 &= 0.525 \pm 0.020 & b_4 &= 0.0185 \pm 0.0019 \\
b_5 &= 15.7 \pm 3.1 & b_6 &= 1.59 \pm 0.07 \\
b_7 &= 1.56 \pm 0.02 & b_8 &= 4.42 \pm 0.18
\end{aligned}$$

The back scattering coefficient is

$$f_{bsct} = 1 + \eta .$$

The energy of the back scattered beta-particle depends on the incident energy and the scattering angle. Because of the continuous energy spectrum of the beta-particles, the two quantities commonly used are the maximum and the average beta energies.^{6,7} For the back scattering approximation one also has to sum and average over the backward angles. Due to the complexity of the analytical calculations involved, for practical applications an empirical relationship was used⁸. This relation is obtained by fitting to a range of beta emitting nuclides of atomic numbers from 10 to 92 and energies from 100 keV to 4 MeV:

$$\frac{E_s}{E_m} = \frac{158 + Z}{251},$$

$$\frac{\bar{E}_s}{\bar{E}} = \frac{123 + Z}{216},$$

where E_s and \bar{E}_s are the energies of the back scattered beta of maximum energy E_m and average energy \bar{E} respectively. The AP0 grab sample is inside a lead container ($Z=82$). Forty percent of the beta-particles back scatter from the lead walls and lose only 5% of their kinetic energy. Ten percent of the beta-particles back scatter from the aluminum backing of the sample-changer's calibration sources and lose about 37% of their energy upon back scattering.

Backscattering of positrons versus electrons f_{β^+}

Based only on single scattering cross section, there is an excess of electrons back scattering over positron back scattering. Experimental results⁹ show a weak Z dependence and an average $\beta^- / \beta^+ = 1.3$. Theoretically calculated value is lower than experimental measurements (1.1 for $Z=80$). Considering these factors, a value of 1.2 was adopted in this paper. The back scattering calculations presented in the previous subsection ignores this effect; therefore, it is included here as a separate factor.

Self – absorption f_{slf_abs}

A sample can absorb some of the beta-particles it emits^{10,11,12,13}. This phenomenon of self absorption depends on the sample thickness and the beta-particle energy. Self absorption will affect the observed counting rate of the sample. It is assumed that beta-particles undergo approximate exponential attenuation, with a half thickness h . The counting efficiency depends on source thickness t , (assuming the source diameter remains constant) and the absorption efficiency is given by

$$\text{Absorption efficiency} = \frac{h}{0.693 t} \left[1 - \exp\left(\frac{-0.693 t}{h}\right) \right].$$

The transmission efficiency is then calculated using

$$F_{\text{slf_abs}} = 1 - \text{Absorption efficiency}.$$

For h (the half value layer in mg/cm^2), it was assumed that it is $\approx 0.1R_0$, where R_0 is the range of the beta-particle. Trajectories of electrons through matter are not straight. Electrons go through large deflections due to their collisions with atomic electrons. As the energy of the electron traversing material increases, energy loss due to radiation increases exponentially. Electrons do not have a well-defined range as do heavier charged particles. Based on empirical data¹⁴, the following relation for the calculation of the ranges of beta-particles has been obtained. This relation is valid for electrons of 10 keV to 3 MeV kinetic energy;

$$R_0(\text{mg} / \text{cm}^2) = 412 E^n$$

$$n = 1.265 - 0.0954 \times \ln(E) ,$$

where E is the beta-particle kinetic energy in MeV.

Window transmission f_{trans}

The fraction of beta-particles transmitted through the GM tube's thin window depends on the window material, thickness and the beta-particle incident energy. The GM tube manufacturer provides a beta-particle transmission graph for the Mica window it uses¹⁵ (see Figure 3). The transmission coefficients were obtained from this graph, for beta energies up to 750 keV (which corresponds to up to 95% transmission) by interpolation. For beta energies above 750 keV, transmission coefficients were obtained by extrapolation.

III. RESULTS

APC system

As a cross check, the efficiency of the GM tube was calculated for several beta emitting standard sources and was compared with the measured values that were obtained from the calibration of the APC wipe counting system¹⁶. The sources were on wipes with aluminum backing with the same diameter as the GM tube, which is 1.75 inches. The source detector separation was 1 ± 0.1 cm. Self absorption in the source material was ignored, since the sources used were extremely thin. The calculated and measured efficiencies are given in Table I;

Isotope	$\bar{E}_\beta (MeV)$	β^\pm	$\epsilon_{calculated}(\%)$	$\epsilon_{measured}(\%)$
^{14}C	0.04947	β^-	3.7 ± 0.2	3.8 ± 3.4
^{22}Na	0.21554	β^+	$15.7 \pm 2.$	14.9 ± 3.3
$^{90}Sr(\rightarrow ^{90}Y)$	0.1958 ->0.9348	β^-	42.0 ± 2.5	40.5 ± 2.4
^{99}Tc	0.08460	β^-	9.9 ± 0.5	9.2 ± 3.2

Table I. Comparison of the measured and calculated efficiencies for beta emitting sources used for APC system calibration.

AP0 lead – pig

The GM detector used for the AP0 measurements had a 1.75” diameter Mica window with an average thickness of 1.7 mg/cm². The lead-pig used for taking grab samples has a right circular cylinder volume of 19.05 cm diameter and 22 cm deep.

Since the distance between the air sample and the GM detector is not fixed, an approximate average value for f_{geom} , was calculated by assuming one thousand distances ranging from zero to 22 cm, for source to detector separation and averaging.

The maximum count rate was about 20 counts per second and this value was used for dead time corrections.

Self absorption coefficient was obtained for the direct beta-particles and for the fraction that was back scattered with the energy \bar{E}_S . A weighted average of the direct and back scattered self absorption factors was used to obtain f_{slf_abs} ,

$$f_{slf_abs} = \frac{1.0 \times F_{slf_abs}(E) + \eta \times F_{slf_abs}(\bar{E}_S)}{f_{bksct}} .$$

Transmission coefficient was obtained for the direct beta-particles and for the fraction that was back scattered with the energy \bar{E}_S . A weighted average of the direct and back scattered transmission factors was used to obtain f_{trans} ,

$$f_{trans} = \frac{1.0 \times T_{direct} + \eta \times T_{backscattered}}{f_{bksct}} .$$

The calculated parameters and efficiencies for the radioisotopes identified in the AP0 grab samples are presented in Table II. Common parameters to all the isotopes are $f_{geom} = 0.1699$ and $f_{dt} = 0.9986$.

Isotope	$\bar{E}_\beta(\text{MeV})$	f_{β^\pm}	f_{bksct}	$f_{slf_abs}(\%)$	$f_{trans}(\%)$	$\epsilon(\%)$
^{13}N	0.4918	β^+	1.413	59.9	91.7	13.2
^{11}C	0.3856	β^+	1.417	49.8	89.0	10.7
^{38}Cl	1.553	β^-	1.435	88.2	99.0	21.3
^{39}Cl	0.821	β^-	1.479	76.3	95.7	18.3
^{41}Ar	0.464	β^-	1.497	57.5	91.2	13.3

Table II. Calculated parameters and efficiencies for the beta emitting isotopes identified in the APO grab sample.

REFERENCES (See the Appendix for copies of references marked with an asterisk.)

- 1.* Technical Associates Stack Monitor Equipment Manual. Fermilab #49779. 7051 Eton Avenue, Canoga Park, CA 91303.
- 2.* Model N1002/8767, TGM Detectors, Inc., 166 Bear Hill Road, Waltham, MA 02154.
- 3.* A. H. Jaffey, *Rev. Sci. Instr.*, 25 (1954), p. 349.
- 4.* A. V. Masket, *Rev. Sci. Instr.*, 28 (1957), p. 191.
- 5.* T. Tabata, R. Ito and S. Okabe, *Nucl. Instr. and Meth.* 94 (1971), p. 509.
6. Bernard Shleien, ed., *1992 The Health Physics and Radiological Health Handbook*.
7. E. Browne and R. B. Firestone, *Table of Radioactive Isotopes* (1986).
- 8.* T. Baltakmens, *Nucl. Instr. and Meth.* 125 (1975), p. 169.
- 9.* H. H. Seliger, *Electron Physics*, NBS Circular 527, 3-17-54.
10. A. H. Snell, ed., *Nuclear Instruments and Their Uses*, Vol. 1 (New York: John Wiley and Sons, 1962).
11. C. V. Robinson, "Geiger-Muller and Proportional Counters," in *Instrumentation in Nuclear Medicine*, ed. G. J. Hine (New York: Academic Press, 1967), p. 57.
12. Watt, D. E. and Ramsden, D. (1964), *High Sensitivity Counting Techniques* (Oxford: Pergamon Press).
- 13.* Measurement of Low-Level Radioactivity, ICRU Report 22 (1979).
- 14.* L. Katz and A. S. Penfold, *Rev. Mod. Phys.* 24 (1958), p. 28.
15. Beta Transmission Graph, TGM Detectors, Inc. 166 Bear Hill Rd, Waltham, Mass. 02154.
- 16.* F. Krueger, *Radiation Physics Note* 96 (1992).

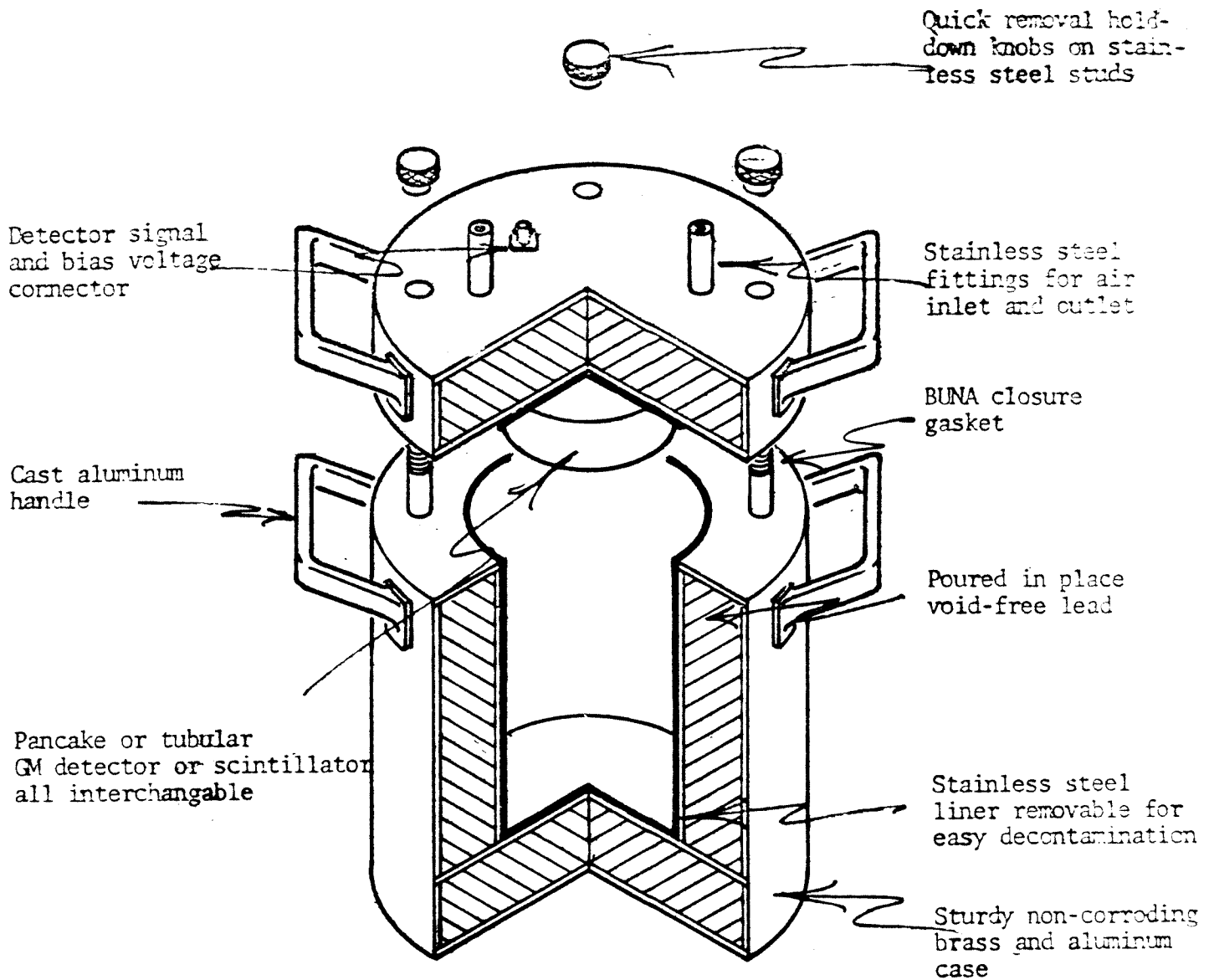


Figure 1. Schematic drawing of the AP0 stack monitor. The walls are 2 inch thick lead. Inside radius of the circular cross section is 9.525 cm. The depth of the cylinder is 22. cm.

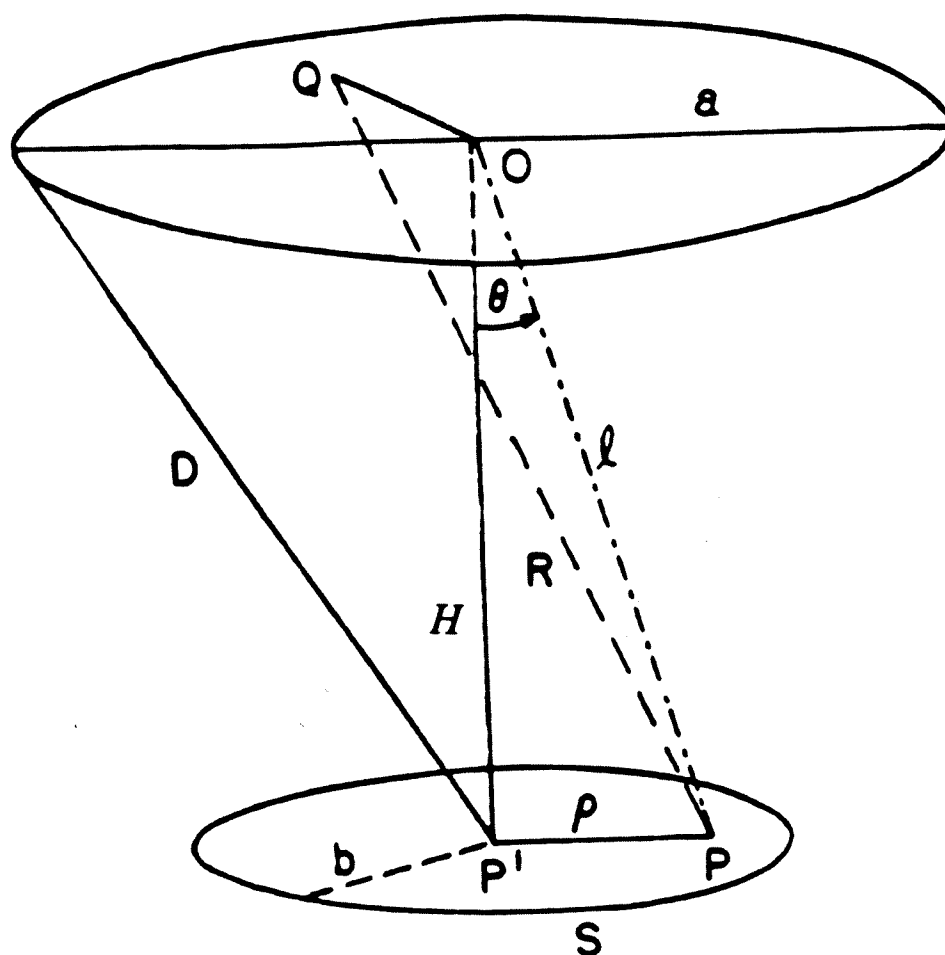


Figure 2. Relation of source and aperture. The upper circle represents the circular aperture to a counter, the lower circle represents a parallel disk source centered on the counter axis. The relevant parameters H , D , a , b are described in the text.

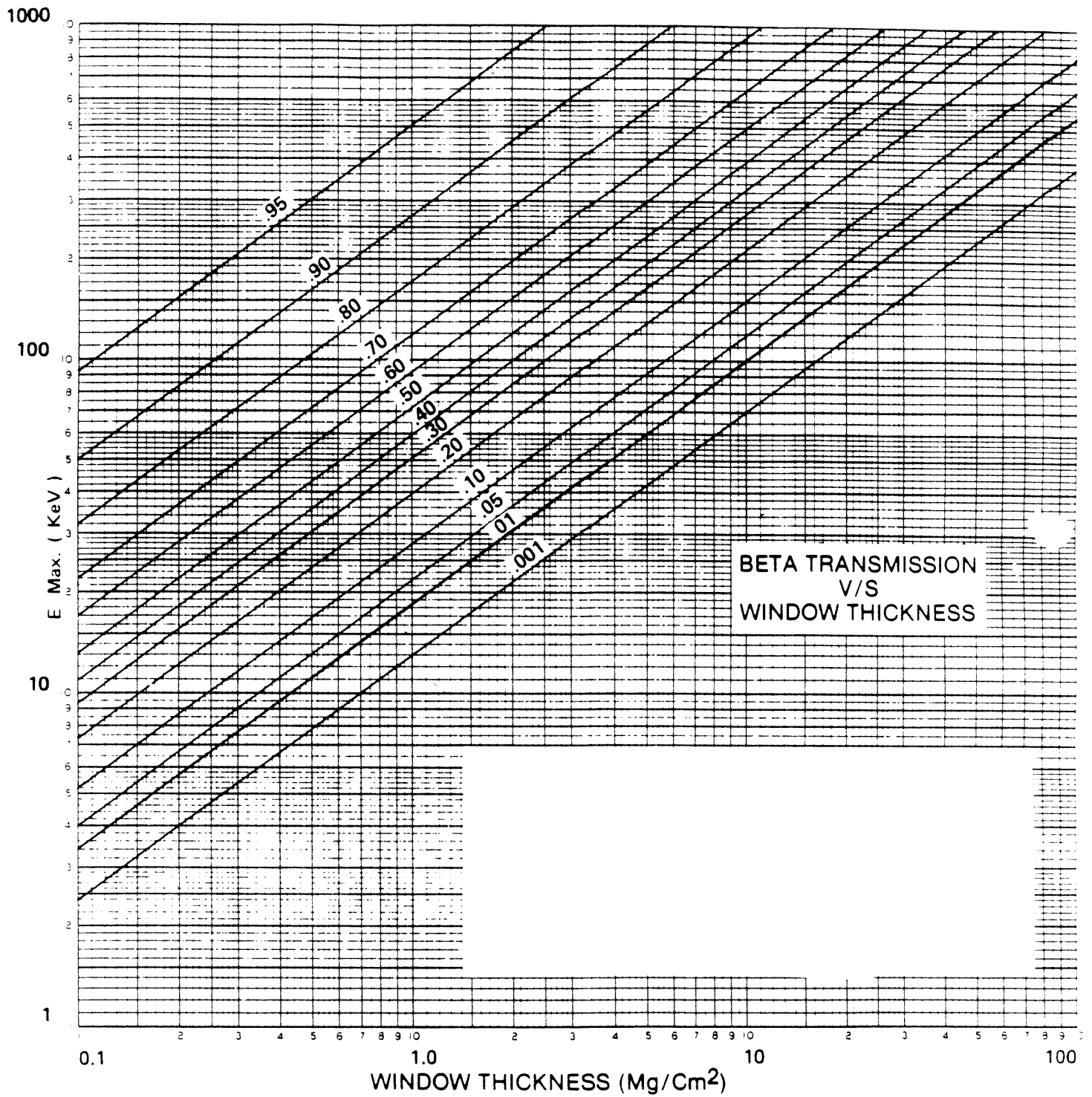


Figure 3. Beta transmission graph as a function of window thickness and beta-particle energy

Appendix